Palaeontologia Electronica
palaeo-electronica.org

Application of micro-CT and SEM-based photogrammetry in the three-dimensional imaging of organic-walled microfossils

Petra Tonarová, Petra Procházková, Marek Zemek, Martina Nohejlová, Ondřej Švagera, Olle Hints, Michal Kubajko, Tomáš Zikmund, and Jozef Kaiser

ABSTRACT

Museum collections are currently undergoing extensive digitisation in the form of three dimensional (3D) imaging of specimens, and palaeontological holdings are no exception. Improved data accessibility brings benefits not only to scientists but also to the general public and science promotion. Microfossils, however, remain a distinct entity in this process because their small size, more complex sample preparation, and higher equipment requirements bring additional challenges. Two representative groups, chitinozoans and scolecodonts, whose average size ranges from 100 to 1000 μm, were chosen to test suitable methods for 3D modelling and imaging of their inner structures. Earlier 3D imaging techniques were predominantly destructive, rendering them unsuitable for type material and other unique specimens. Our main objective was to introduce and test two 3D modelling approaches appropriate for the online presentation of museum collections, and to develop a repeatable sample preparation protocol for future studies. X-ray computed tomography (CT), specifically micro-CT and submicron-CT (CT with achievable resolution in the micrometre and sub-micrometre range, respectively), and microphotogrammetry based on scanning electron microscopy (SEM) images were applied. In addition, the acquired 3D models can be used for science outreach and educational purposes, including the production of 3D-printed models.

Petra Tonarová. Czech Geological Survey, Klárov 3/131, 11800 Praha 1, Czech Republic. petra.tonarova@geology.cz
Petra Procházková. CEITEC—Central European Institute of Technology, Brno University of Technology, Brno, Czech Republic and Department of Soil Science and Plant Nutrition, Faculty of AgriSciences, Mendel University in Brno, Zemědělská 1, 613 00 Brno, Czech Republic. petra.prochazkova@mendelu.cz
Marek Zemek. CEITEC—Central European Institute of Technology, Brno University of Technology, Brno, Czech Republic. Marek.Zemek@ceitec.vutbr.cz
Martina Nohejlová. Czech Geological Survey, Klárov 3/131, 11800 Praha 1, Czech Republic martina.nohejlova@geology.cz

Final citation: Tonarová, Petra, Procházková, Petra, Zemek, Marek, Nohejlová, Martina, Švagera, Ondřej, Hints, Olle, Kubajko, Michal, Zikmund, Tomáš, and Kaiser, Jozef. 2026. Application of micro-CT and SEM-based photogrammetry in the 3D imaging of organic-walled microfossils. Palaeontologia Electronica, 29(2):a32.
https://doi.org/10.26879/1659
palaeo-electronica.org/content/2026/5926-photogrammetry-in-the-3d-imaging-of-microfossils

Ondřej Švagera. Czech Geological Survey, Klárov 3/131, 11800 Praha 1, Czech Republic
ondrej.svagera@geology.cz
Olle Hints. Department of Geology, Tallinn University of Technology, Ehitajate tee 5, 19086 Tallinn, Estonia.
olle.hints@taltech.ee
Michal Kubajko. Czech Geological Survey, Klárov 3/131, 11800 Praha 1, Czech Republic.
michal.kubajko@geology.cz
Tomáš Zikmund. CEITEC–Central European Institute of Technology, Brno University of Technology, Brno, Czech Republic. Tomas.Zikmund@ceitec.vutbr.cz
Jozef Kaiser. CEITEC—Central European Institute of Technology, Brno University of Technology, Brno, Czech Republic. jozef.kaiser@ceitec.vutbr.cz

Keywords: fossil collection digitisation, 3D modelling, non-destructive methods, submicron computed tomography, scolecodonts, chitinozoans

Submission: 26 November 2025. Acceptance: 14 July 2026.

INTRODUCTION

Substantial portions of natural history collections, including palaeontological collections, represent ‘dark data’ that remain effectively hidden from broader scientific use and public access. Digitisation efforts, the FAIR principles (findable, accessible, interoperable, reusable) for data publishing, and virtual repositories have improved the situation in recent decades, increasing access to material that would otherwise be unavailable due to space limitations, logistical constraints, etc. Freely available digital data offer substantial scientific and economic benefits, including time efficiency and reduced travel costs (Popov et al., 2021). Digitisation has evolved over the years from simple digital photography to the development of databases of digital 3D models accompanied by metadata (locality, stratigraphy, lithology, repository, etc.), providing a robust foundation for further analysis.

Digitising microfossils, however, is challenging because of their small size and fragility. Light microscopy and scanning electron microscopy have been the primary imaging techniques for microfossils for decades (Kielan-Jaworowska, 1966; Combaz et al., 1967; Jansonius, 1967; Eriksson et al., 2004, 2013). Light microscopy, used since the beginnings of micropalaeontological research, is limited by a shallow depth of field. Deep-focus techniques (‘focus stacking’ or ‘z-stacking’) can introduce potential artefacts into microphotographs. Standard digital cameras mounted on optical microscopes now offer a resolution of 25 to 50 megapixels. Scanning electron microscopy (SEM), provides higher resolution, depth of focus, and magnification of microphotographs (Hay and Sandberg, 1967). SEM microphotographs can also be used for focus stacking and 3D anaglyphs, but these approaches remain uncommon and reveal only one side of the specimen (Jarochowska et al., 2013; Cypionka et al., 2015).

The main goal of the present study was to test methods for 3D visualisation of microfossils. Scolecodonts and chitinozoans were selected as representative examples due to their abundance and diversity in lower Paleozoic microfossil assemblages and the important role of chitinozoans in stratigraphy. These groups lived under different palaeoecological conditions; scolecodont-bearing polychaetes were components of the benthic fauna, whereas chitinozoans represent planktonic or epiplanktonic organisms. Both groups played important roles in early Paleozoic marine ecosystems.

Studied Microfossils

Scolecodonts. Scolecodonts are components (jaw plates and simple teeth) of the complex jaw apparatus of mainly eunicid polychaetes. These microfossils are common, especially in lower Paleozoic sediments worldwide (Eriksson et al., 2013) but can be found in younger sediments up to the recent. They are often the only part preserved from otherwise soft-bodied worms. Their scleroprotein composition makes them chemically resistant and enables their extraction from rocks by acid maceration (Eriksson et al., 2013). Combined research on fossil and recent jaws has found that they are useful for inferring evolutionary relationships among polychaetes (Paxton, 2009; Hints et al., 2017).

The study of the internal structure of scolecodonts used to be more complicated, and the methods employed were often destructive. Transmission electron microscopy (TEM) and SEM of broken specimens have been commonly applied (Strauch, 1973; Corradini et al., 1974; Mierzejewska and Mierzejewski, 1975, 1977, 1978, and references therein). Tasch and Shaffer (1961) and Schwab (1966) studied bleached recent and fossil scolecodonts using transmitted light. They found that the jaws were composed of two layers: first, a dense, lamellar, dark-brown to black organic-rich outer layer and second, a less dense, light-brown inner layer with common minute tubules. Nevertheless, this method was also harmful to the specimens because they became not only translucent but also very fragile.

Only a few studies have used computed tomography (CT) to study the fossil polychaete jaws. Eriksson et al. (2017) used CT to reconstruct the maxillae embedded in rock. They studied the oldest 'Bobbit worm' from the Lower-Middle Devonian of Ontario, Canada. These maxillae are the largest known scolecodonts, measuring over a centimetre in length. This contrasts with the 'normal' size of scolecodonts, which ranges from 200–300 µm to 1,000 µm in length (Eriksson et al., 2004). This range is below or on the limit of what can be scanned by micro-CT devices (Keklikoglou et al., 2019; Heřmanová et al., 2023). Recently, Tonarová et al. (2024) used submicron-CT to study fossil scolecodonts and created 3D models of the maxillae. These images and videos provide additional information about the new species and genus, including the inner structure of the maxillae.

Parry et al. (2019) used micro-CT to study body-fossil polychaetes. They reconstructed the maxillary apparatus of *Plumulites* (machaeridian) and confirmed a long-disputed position of machaeridians within the crown group of the Phyllodocida (sister group of Eunicida). Thanks to micro-CT analysis, Gueriau et al. (2023) resolved the genuine affinity of *Gilsonicaris rhenanus* Van Straelen, 1943 from the Lower Devonian Hunsrück Slate, Germany. Previously, this species was thought to belong to anostracan crustaceans. Micro-CT scanning combined with X-ray radiography revealed new anatomical details, including four pairs of jaws morphologically consistent with those of scolecodonts in eunicean polychaetes.

Fossil polychaete worms have living relatives whose soft tissues can be examined and scanned (Dinley et al., 2010; Faulwetter et al., 2013). The latter authors focused on the potential and limitations of virtual type material (cybertypes) and the establishment of virtual collections. A recent study by Clemo and Dorgan (2017) employed a novel method to investigate living jawed polychaetes, with a primary focus on their maxillary apparatuses. Using computed tomography, they created 3D-printed models and analysed the functioning principles of the jaw apparatuses based on these models, focusing on the connection with the worms' diet.

Chitinozoans. Chitinozoans are composed of enduring organic matter (Jacob et al., 2007) and can commonly be found in lower Paleozoic marine sedimentary rocks worldwide. The affinity of chitinozoans remains a topic of debate. They are interpreted either as eggs of marine metazoans or as individual microorganisms (Liang et al., 2020; Vodička et al., 2022). Nevertheless, their uncertain affiliation does not prevent them from being an important stratigraphic tool (e.g., Paris, 1990; Grahn, 2005, 2006).

Similarly to scolecodonts, chitinozoan internal structures were mainly studied using SEM on broken or dissected specimens (Urban, 1972; Laufeld, 1974; Wrona, 1980; Bockelie, 1981) or by bleaching, when the transparent vesicle was studied under a transmitting light microscope. The results of these early investigations were summarised by Combaz et al. (1967), who concluded that a chitinozoan vesicle wall could consist of one, two, or even three layers: the outer 'periderm', middle 'ectoderm', and inner 'endoderm'; the inner layer could be confined to merely some portions of the vesicle wall. Similar conclusions were commonly drawn from infrared video microscopy (Jansonius, 1964, 1967; Urban, 1972; Umnova, 1973; Laufeld, 1974; Melchin and Anderson, 1998) and SEM studies (Urban and Kline, 1970; Urban, 1972; Laufeld, 1974). In contrast, Eisenack (1968, 1972, 1976), who applied not only the above-mentioned methods but also a TEM, recorded a homogeneous, unilayered vesicle wall in all chitinozoans he studied. However, all these methods were destructive.

More recently, Wang et al. (2021) combined the argon ion/milled backscatter SEM imaging method with micro-CT. In this case, the main focus was on the carina of the genus *Cyathochitina*. They found that the carina was loosely filled with sponge-like fibers of similar chemical composition to the main vesicle layers. The carina offered two benefits: firstly, it strengthened the basal firmness and reduced the weight of the chitinozoan vesicle by filling it with spongy fibrils, and secondly, computational fluid dynamics (CFD) analysis suggests that the formation of the carina might have improved the hydrodynamic properties and floating ability of the vesicle by dispersal in different hydrodynamic regimes. Liang et al. (2020) applied near-infrared microscopy (NIR), focused ion beam scanning electron microscopy (FIB-SEM) analyses, field emission scanning electron microscope, and CT to support the idea of chitinozoans as the reproductive stages of distinct microorganisms.

Submicron Computed Tomography – Previous Application in Palaeontology

Computed tomography has been widely used in palaeontology in the last decade (see Abdelhady et al., 2024 for a review of its history). Abel et al. (2012) created a methodological summary of how to prepare 'virtual' fossils. The undisputable advantage of the method is its non-destructive character, which provides new insight into the study of ultrastructure. The micron- and submicron-scale studies of fossils are still in progress. For example, conodonts have been studied by these methods, especially in the last 10 years. They have complex jaw apparatuses composed of calcium phosphate (similar to teeth and bones of vertebrates). For example, Suttner et al. (2018) used CT to study the *Icriodus* cluster, they discussed the wearing of the conodont tips, and reconstructed the motion model of the apparatus. Souquet et al. (2020a, 2020b) studied Carboniferous conodonts using micro-CT and produced 3D models of the new species they described. Girard et al. (2022) used 2D and 3D (based on micro-CT models) biometric and geometric morphometric analyses to test ontogenetic changes among platform elements of *Icriodus* species.

Photogrammetry – Previous Application in Palaeontology

Photogrammetry is a well-established method that has been used by geographers for more than 160 years. This method works by constructing a 3D model from multiple photographs taken from different angles (Surmen, 2023). The basic principle behind all photogrammetric measurements is the geometrical–mathematical reconstruction of the paths of rays from the object to the sensor at the moment of exposure. Photogrammetry comprises all techniques concerned with making measurements of real-world objects and terrain features from images. These may be aerial as well as terrestrial images, and they may be taken by film cameras, digital cameras, or electronic scanners on tripods, airborne, or spaceborne platforms. Applications include measuring of coordinates, quantifying of distances, heights, areas, and volumes, preparing topographic maps, and generating digital elevation models and orthophotographs (Aber et al., 2010; Falkingham, 2012; Bemis et al., 2014).

With rapid advancements in software and hardware capabilities in recent decades, it is now used not only to create 3D landscape models but also to model nearly any object that can be photographed. In palaeontology, photogrammetry has predominantly been applied to dinosaur tracks (Breithaupt and Matthews, 2001; Matthews et al., 2006; Bates et al., 2009) and to vertebrate palaeontology in general. Otero et al. (2020) made a compilation of surface scanning techniques for 3D acquisition used in vertebrate palaeontology. Both methods, laser scanning and photogrammetry, have their pros and cons. Laser scanners are rather expensive and can be used for bigger objects. On the other hand, photogrammetry often has to involve the use of numerous markers within the photographs and subsequent post-processing with expensive commercial packages that can require considerable user input to select matching points and align the photographs. Therefore, its cost rises due to the price of proprietary software and the required expertise (Falkingham, 2012; Cunningham, 2021).

The SEM-microphotogrammetry has been reported already by e.g., Boyde and Ross (1975), but it has never been applied on a routine basis. Eulitz and Reiss (2015) presented a simple, and non-destructive method for 3D surface reconstruction from SEM samples based on the principles of optical close-range photogrammetry. A series of overlapping photos was used to generate a 3D model of the surface of an object. Instead of moving a detector around the object, the object itself was rotated. A series of overlapping photos was stitched and converted into a 3D model using the software commonly used for optical photogrammetry. A rabbit kidney glomerulus was used to demonstrate the workflow of this adaptation. The reconstruction produced a realistic high-resolution 3D mesh model of the glomerular surface.

Gontard et al. (2016) developed a methodology for the high-resolution 3D reconstruction of the surface and texture of $LiTi_2(PO_4)_3$ particle (ca. 5 μm) in the SEM using photogrammetry. The 3D models were created using Meshlab freeware to measure geometrical parameters from the 3D model. The data were used for 3D printing to visualise the reconstructed model. However, microfossils have not been used to test the method and to develop a repeatable procedure. Ball et al. (2017) compared common non-destructive techniques for acquiring 3D data for microscopic and macroscopic samples. They compared micro-CT, confocal microscopy, surface scanning, Z-stacking, and photogrammetry. Submicron and micro-CT are the most widely used methods to acquire three-dimensional microfossils. However, the limitation lies in the price of the technique. Therefore, Ball et al. (2017) applied structure-from-motion photogrammetry using SEM photographs. The SEM photodocumentation was programmed using macros to automatically capture dozens of images at suitable angles to generate accurate 3D reconstruction (with controlled stage requirements such as sample height, centre of rotation, and tilt centre calibration). Afterwards, the software Agisoft software was used to obtain 3D surface models with micron-scale resolution that can be exported as polygon meshes and eventually 3D printed. For testing, they used different objects, diatoms, butterfly scales, and mineral fabrics. The high resolution was emphasised as an advantage of this method.

Kozikowski (2020) applied optical photogrammetry using SEM images to obtain 3D models and quantitative data on carbon particles and graphite nanoparticles. The image acquisition was automated by the external macro software. Mesh data were reconstructed from a number of images taken at multiple sample stage tilt angles with a supplementary measurement of TEM grids for method validation. This 3D model has been scaled and processed to obtain values such as the volume, height, and surface area of the samples and has been quantitatively compared with 2D measurements.

Dumitriu et al. (2021) described a method for the microfossil representation. The method allows for more accurate measurement of the specimens` morphology. The structure-from-motion photogrammetry technique makes use of a very accessible methodology: SEM photos and photogrammetry software. The 3D models have been made for nine specimens of foraminifera, ostracods, radiolarians, ascidian spicules, and dinoflagellate cysts. The variability of the studied specimens proved that this method can be successfully applied to almost all groups of microfossils.

However, studies on photogrammetry based on SEM microphotographs of organic-walled microfossils have been missing so far.

MATERIALS AND METHODS

Microfossils Samples

The microfossils, namely scolecodonts and chitinozoans, from the Ordovician of India (more information in Tonarová et al., 2024), Silurian rocks from Estonia and the Prague Basin (Czech Republic) were used in this study. The following localities were sampled: the Reinu Quarry in Estonia (coordinates 59.087299, 24.73768), Sutlema Quarry in Estonia (59.174096, 24.619575), and the Kosov Quarry in the Czech Republic (coordinates 49.936722, 14.055583). Rock samples were dissolved in 6% acetic acid, and the insoluble residue was sieved through a 50 µm mesh. The microfossils were hand-picked from a wet residue using a micropipette (Kielan-Jaworowska, 1966). Different mounting methods were used for the imaging techniques (details below). The microfossils are housed in the collections of the Czech Geological Survey in Prague, under collection numbers PT169, PT171–176.

Submicron Computed Tomography

For the submicron-CT, several methods of specimen mounting were tested: the sample was placed in a block of polystyrene (i), mounted directly onto a sample holder (ii), mounted in a Kapton tube (iii), and in a pipette tip (iv).

Using a polystyrene (i) is a standard mounting strategy in micro-CT for larger specimens. In this case, the microfossil was placed in a pre-prepared notch in a polystyrene block glued to the sample holder prior to micro-CT measurement. In the case of mounting the sample directly onto a sample holder (ii), the microfossil was glued on a kapton layer containing a reference steel sphere using a thin layer of water-soluble dispersion glue (Herkules). When using the Kapton tube (iii), microfossils were placed inside a tube attached to the sample holder, and the tube was sealed with parafilm foil. The tube can be attached to the top of the holder using glue or fitted over it.

Finally, a new sample preparation strategy (Figure 1) was tested to mitigate the difficulties described above, using a small pipette tip instead of a Kapton tube (iv). The narrow opening of the pipette tip was covered by a permeable material, such as filter paper, to catch solid materials in the tip while allowing fluids to pass through. Microfossils were inserted through the wide opening of the tip, which was significantly simpler than the same procedure performed with the narrow Kapton tube. Similar to Kapton, the plastic of the pipette tip is

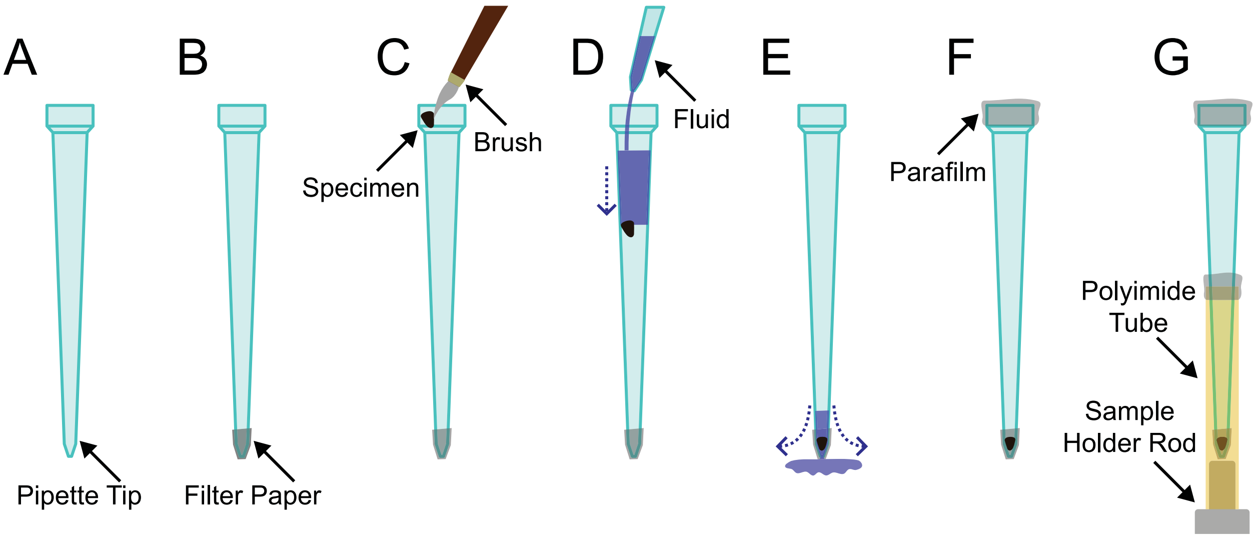

FIGURE 1. New methodology of mounting specimens for computed tomography scanning using a pipetting tip. A. The plastic pipette tip. B. The narrow opening of the pipette tip was covered by a permeable material (filter paper), fixed in place by a piece of tape. C. Microfossils were inserted through the wide opening of the tip using a fine brush. D. The microfossils were washed down to the narrow tip using water or ethanol. E. The excess fluid was drained through the cover on the narrow end and soaked up by fabric or filtration paper; any residual liquid was left to evaporate. F. The top of the pipette tip was covered with parafilm foil to prevent the loss of microfossils during manipulation. G. The pipette tip was affixed to a sample holder rod, with the narrow side facing down. The position of the pipette tip was supported and secured by a Kapton tube and parafilm.

sufficiently radiolucent for X-ray imaging, but stable enough to serve as a sample container. Once inserted, the microfossils were washed down to the narrow tip using water or ethanol. The excess fluid was then soaked up by fabric or filtration paper, and any residual liquid was left to evaporate. Washing the samples down into the narrow portion of the tip ensures that the samples fit into a small volume, which facilitates high-resolution CT scans with a small field of view. After that, the top of the pipette tip was covered with parafilm foil to prevent the samples from falling out of the tip during manipulation. Finally, the tip was fixed to a holder with the narrow side facing down.

After mounting, the microfossil samples were scanned using a Rigaku Nano3DX submicron-CT scanner (Rigaku Corporation, Japan). The Nano3DX uses a MicroMax-007 HF X-rays generator with switchable copper (Cu) and molybdenum (Mo) targets operating at tube voltages and currents of 40 kV/30 mA and 50 kV/24 mA, respectively. The Cu target provides superior contrast in X-ray images of relatively radiolucent samples, while the Mo target improves X-ray penetration in more radio-opaque materials. X-ray projection images are captured using an XSight Micron LC X-ray detector equipped with a scintillator, 20× magnifying microscope optics, and an 8.25-megapixel charge-coupled device sensor with a size of 3300×2500 pixels, which corresponds to a minimum achievable effective pixel size of 270 nm.

Settings of the CT scan depend on the composition of the scanned samples. In this work, scans of both scolecodonts and chitinozoans constituted 800 projection images in a 180° angular range, and pixel binning with a factor of 2, which increased the effective pixel size of acquired images to 540 nm while also increasing the signal-to-noise ratio and reducing acquisition times.

The scolecodont samples included a thin metallic coating from prior SEM imaging, which increased the radio-opacity of the samples during the subsequent CT scan, so the Mo target was used, and a 0.1 mm aluminium filter was placed in front of the X-ray generator to increase the mean X-rays energy. X-ray filtration mitigates the so-called beam hardening artefacts, which are a common issue in X-ray imaging of metals and other heavy materials. Exposure time per projection was set to 6 seconds, leading to a scan time of 1 hour and 35 minutes. The detector was placed at a distance of 3 mm from the sample, facilitating the application of propagation-based phase contrast.

Samples of chitinozoans were scanned natively (without any additional staining or coating), so the Cu target was used for increased contrast.

No additional filtration of the X-ray beam was used, and the detector was placed to within 1.75 mm of the sample to minimise image blur. The exposure time was set to 8 seconds per projection, resulting in a scan time of 2 hours and 2 minutes.

Volumetric CT datasets were reconstructed from the acquired raw projection data using Rigaku's CTReconstructionApp, version 2.1.2.0. Further processing and analysis of the volumes, including segmentation, visualisation, and wall thickness analysis (Figures 2– 5, Appendices 1–9, 17–19), were done in VGStudio MAX 2023.1 (Volume Graphics, Germany).

Photogrammetry

The scanning electron microscope FEG-SEM Tescan Mira 3GMU (at the Czech Geological Survey, Prague), equipped with an eucentric table, was used to acquire images of microfossils. Between 25 to 50 microphotographs of each specimen were taken manually (rotating the table and scanning the specimen from all sides and angles). In the first attempt, the specimen was glued on the dorsal side, gold-coated, scanned, unglued, and glued again from the ventral side, gold-coated for the second time, and scanned again. That means that each specimen was transferred twice. In the second attempt, the specimen was carefully stuck to the carbon tape on the SEM stub with its very end (Figure 6), and then documented from different angles, which required only one transfer of the specimen.

Agisoft Metashape Professional version 1.8.4 (build 14856) was used to create photogrammetric models from SEM images (Appendices 10–16). The program creates spatial objects (point clouds) based on the structure from motion method, which uses the relative positions of the images taken to identify and calculate the shape of the object being studied (Figure 7). Finally, the surface is covered with a photo texture generated from the original images. The object can then be scaled to real size, ensuring its use for analytical purposes. To successfully create a 3D model from SEM, it is necessary to take at least 50 photographs with a 50% overlap or more, capturing the object from all sides. In the case of limited SEM scanning possibilities, the object must therefore be positioned appropriately (positioning the object on its height, placing it on its top and bottom edges, etc.). Then the background of the image must be removed, which introduces distorting information into the structure from motion process and makes it impossible to assemble the object correctly.

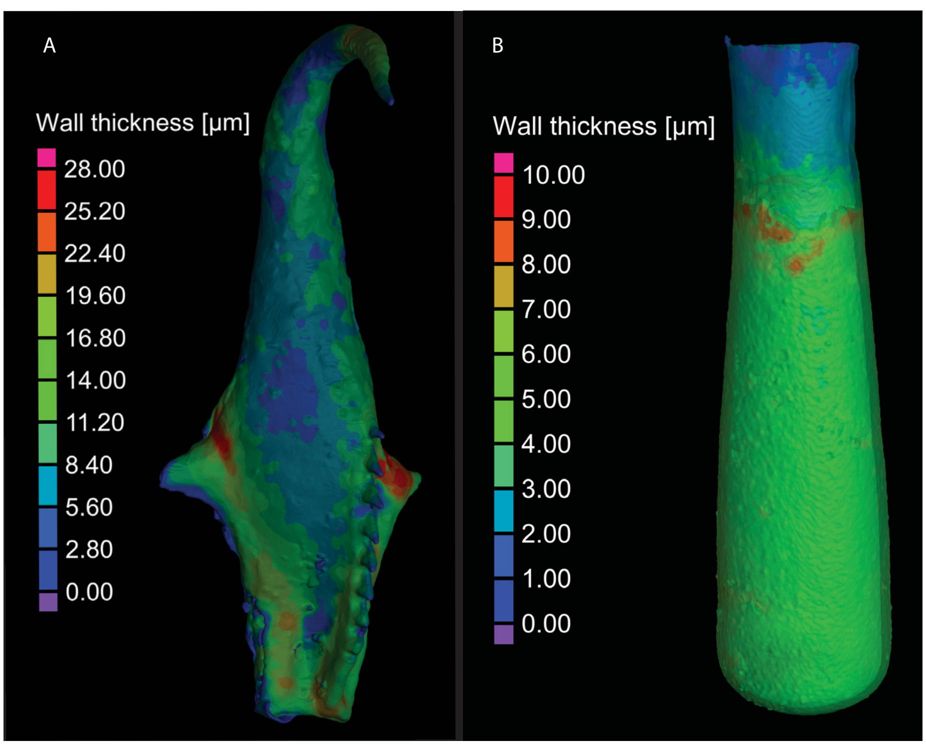

FIGURE 2. Wall thickness analysis. A. *Spitiprion khannai,* left MI, specimen PT169_1, India, Ordovician Spiti Formation. B. Chitinozoa, specimen PT175_3, from sample OM12-6, Sutlema Quarry, Estonia, Saunja Formation, Katian, Estonia.

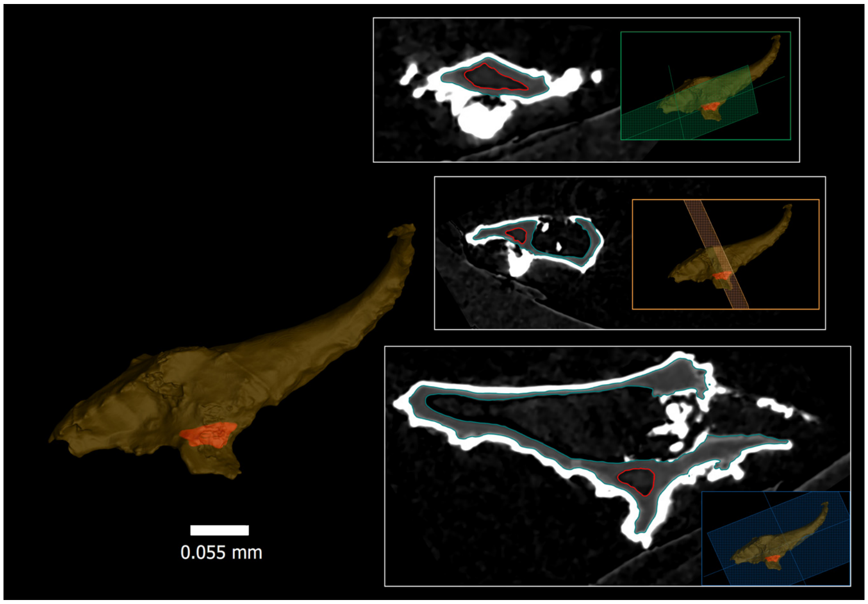

FIGURE 3. Voids in the right first maxilla of *Spitiprion khannai*, left MI, specimen PT169_2, India, Spiti Formation. The voids are highlighted in red. The three insets on the right show slices through the specimen in three orthogonal color-coded planes.

RESULTS

Submicron Computed Tomography

The first chosen approach (i) was attempted because polystyrene is soft enough not to crush the sample, but rigid enough to keep it steady. However, handling of the prepared sample and any subsequent adjustments to its position are difficult. Dismounting the sample can also be problematic, as it requires careful manipulation of the polystyrene.

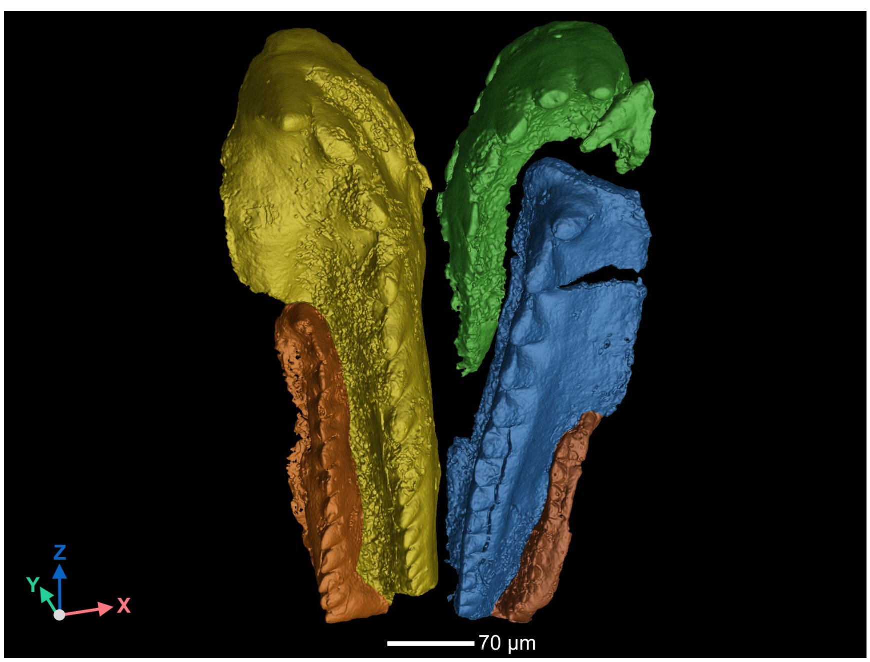

FIGURE 3. Voids in the right first maxilla of *Spitiprion khannai*, left MI, specimen PT169_2, India, Spiti Formation. The voids are highlighted in red. The three insets on the right show slices through the specimen in three orthogonal color-coded planes.

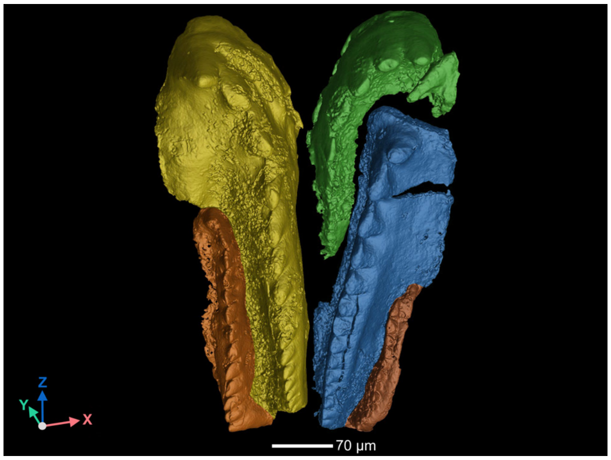

FIGURE 4. Fused maxillary apparatus of *Pistoprion transitans* (specimen 176_1), image acquired by CT scanning. The maxillae can be virtually moved (see Appendix 3). Yellow = left first maxilla (MI), blue = right MI, green = second maxilla, red = lateral teeth. Sample from Reinu Quarry, Silurian, Varbola Formation, Estonia.

In the second tested method (ii), the thin layer of water-soluble glue had the tendency to dry quickly, which put a stringent time limit on mounting the samples onto the holder. In some cases, the glue had mostly dried before the sample was placed on it, which placed the fossil at risk of being lost or damaged due to insufficient adherence to the holder, and it increased the possibility of sample movement (and thus reduced data quality) during the CT scan. This issue can be mitigated by applying a thicker layer of glue, but this, in turn, complicates data processing and analysis. When the glue and the microfossil have similar X-ray attenuation, one can conceivably be misidentified as the other in CT data, which has the potential to skew the shapes of extracted 3D models of microfossils. If the glued fossil adheres sufficiently to the holder, it is very secure and conducive to stable CT measurements, while being relatively straightforward (if time-consuming) to dismount by applying water to dissolve the glue.

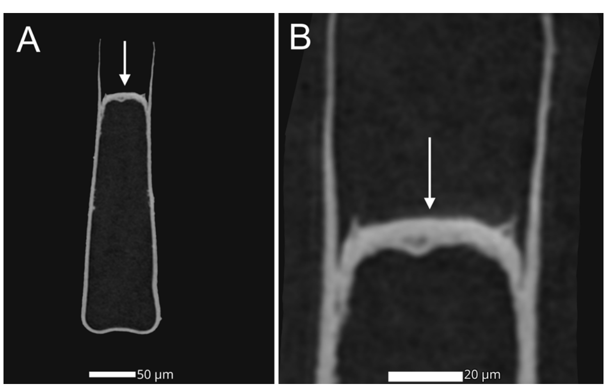

FIGURE 5. Detail of the chitinozoan prosome (pointed by the arrow), visible on the CT scan, specimen PT175_3, from sample OM12-6, Sutlema Quarry, Estonia, Saunja Formation, Katian. A. The whole chitinozoan. B. Magnified detail of the prosome.

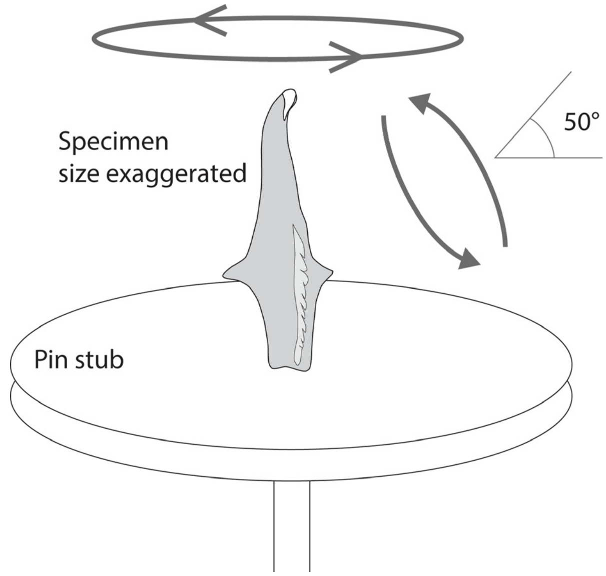

FIGURE 6. Scheme of the specimen (microfossil) mounted by a carbon adhesive disc to the SEM pin stub. The microphotographs are taken all around the specimen and the pin stub is being tilted during the process, the photographs are further processed by photogrammetry.

When using a Kapton tube (iii) for microfossil sample mounting, inserting microfossils into the tube requires more effort compared to other techniques due to the small opening of the tube. However, once the sample is prepared, it can be handled without much risk of damaging the specimens. The samples themselves are relatively secure and resistant to movement during the measurements without the need for adhesives (which is beneficial for data processing), although they may still move when subjected to strong vibrations or manipulation with the sample holder. This method of sample preparation is also very convenient for scanning multiple samples at once, as the Kapton tube securely contains all specimens in a small volume, which can be effectively positioned within the field of view of a CT scan. In such cases, however, the diameter of the tube must be selected carefully to fit within this field of view.

Finally, the best option, which mitigates the difficulties described above, was the use of a small pipette tip (iv) instead of the Kapton tube (Figure 1). This method avoids using potentially problem-

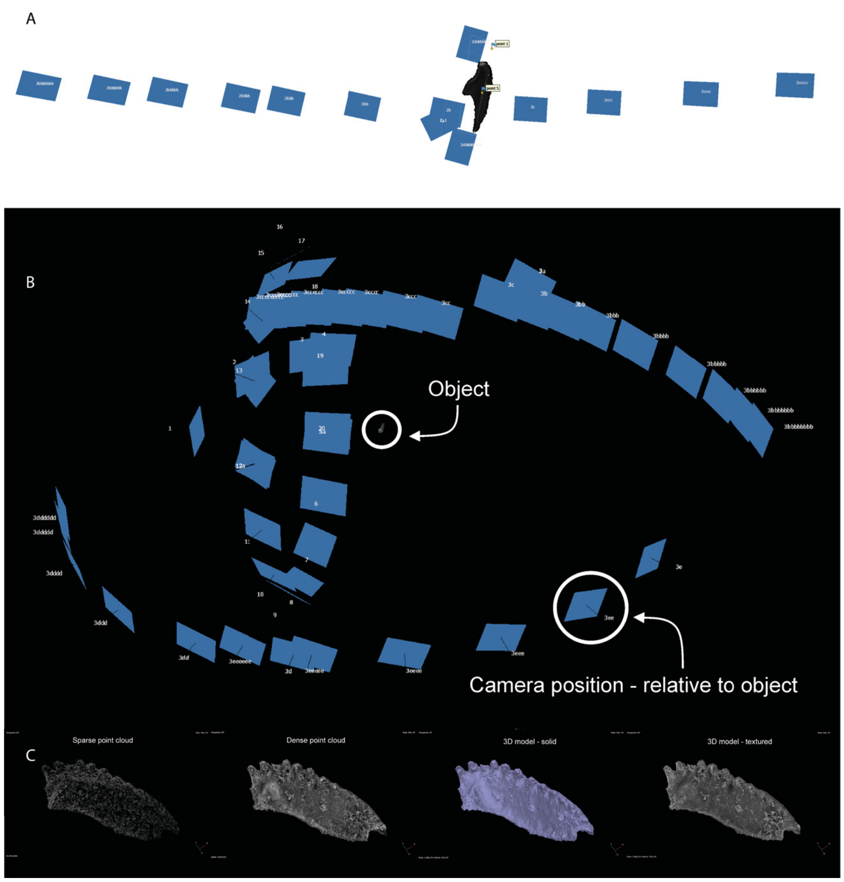

FIGURE 7. Photogrammetry procedure. Object position, as perceived by the Metashape software, relative to the source image taken from scanning electron microscopy (SEM). A. Close-up image of the modelled object. B. The whole object surrounding with camera (SEM) position. C. 3D model building workflow showing from left to right the sparse point cloud created directly from SFM (SEM images) containing 31 655 points capturing the object geometry, dense point cloud (densified sparse point cloud) consisting of 4 563 623 points and resulting triangulated 3D model, untextured and textured using 1 006 332 triangulated faces.

atic adhesives, facilitates the collection of multiple specimens in a small volume for more efficient CT scanning, and allows a relatively fast and straightforward dismounting and recovery of the samples.

Time load: approx. 1 hour of calibration and 2 to 5 hours of measurements, followed by 1 to 2 hours of software reconstruction with Rigaku software and processing with the software VGStudio MAX 2023.1 (Volume Graphics, Germany).

Photogrammetry

The first test attempt, in which the microfossil sample was repeatedly glued and gold-coated, proved risky, and one of the samples broke during the process. The second technique, which involved sticking microfossils to the carbon tape on the SEM stub in a 'standing' position (on one tip of the microfossil) - brought much better results, both in the coverage of the specimen-surface from almost all views, and treatment with the samples was far less harmful. The best results were gained with at least 30 SEM microphotographs.

For holotypes or type microfossil collections, the recommended method is SEM-based photogrammetry. In our study, we used Agisoft Metashape Professional version 1.8.4 to create 3D models from SEM images of scolecodonts and chitinozoans. The advantages of this method are its low cost (aside from the software and working hours of the operator) and rapid model computation, depending on the hardware specifications. The high-resolution microphotographs for holotype description are produced during the modelling process. The 3D models are especially beneficial for fossils with diagnostic features on both the ventral and dorsal sides.

The photogrammetry reconstruction faced some challenges. It has turned out that the simple and conical shape of chitinozoans is more complicated to process than the more diverse surface of scolecodonts. The ‘body’ of chitinozoans is cylindrical in shape and very similar from all sides, with few distinct markings (Figures 8, 9, Appendices 14, 16). Photogrammetry reconstructions often struggle with objects such as spheres or cones, as the method has difficulty finding distinct markers on the object, which can be related to its specific side, e.g., dorsal/ventral. This issue can be resolved by adding additional images of the problematic part of the object, although it requires mounting the specimen and repeating the SEM procedure.

The majority of the time load is devoted to SEM scanning (approximately 1 hour per specimen) and image adjustment (processing of images using Adobe Photoshop, 1–2 hours per specimen). Therefore, the cost can be estimated at approximately 50 EUR (price for an hour of SEM). The limitation of the method is that it captures only the external structure of objects, requiring careful photography from multiple angles with at least 50% overlap to ensure complete surface coverage.

DISCUSSION AND CONCLUSIONS

This study set out to extend the current efforts in the digitisation of museum collections to 3D imaging of delicate microfossil specimens. Two complementary imaging approaches, micro-CT and SEM-based photogrammetry, were tested. We have compared the time, price, and gained results for 3D models of chitinozoans and scolecodonts. The SWOT (Strengths, Weaknesses, Opportunities, Threats) analysis presented in Figures 10 and 11 highlights that both methods have distinctive advantages, as well as inherent constraints and trade-offs. A nuanced interpretation of the present findings, therefore, requires careful consideration of these aspects to facilitate the informed selection of the most suitable technique – or an integrated application of both – in addressing specific research objectives.

SEM-based photogrammetry proved to be an efficient and accessible technique for imaging the surface morphology of microfossils, producing highly detailed 3D models of microfossils with diverse and complex surface features (Figure 8). When using high-resolution equipment, it is possible to display exceptional surface detail at a level comparable to laser scanning, particularly for macroscopic objects. It has been shown that photogrammetric reconstruction works better when samples have a more complex structure with more morphological markers, because smooth, reflective, or spherical surfaces are challenging to capture due to a lack of unique visual features. This limitation can be mitigated by acquiring additional images of problematic regions, though this requires remounting the specimen and repeating the procedure. When dealing with minor inconsistencies, such as gaps or overlapping parts, additional markers can be attached to specific locations in the source photographs within Agisoft Metashape. This helps the algorithm better pair and align the images, ultimately leading to improved overall geometry. While we tested this approach and achieved better results, they were still not entirely acceptable. Further refinement of the resulting 3D solid (wireframe) model can be achieved using the built-in smoothing and decimation functions. Both can yield decent results; however, we strongly recommend using small increments when adjusting these settings and always working on a duplicate of the original model. In our case, we manually extracted any floating points in the dense cloud to achieve the resulting solid model. Despite aforementioned constraints, the resulting photogrammetric models are suitable for scaling, exporting in standard formats (e.g., STL, OBJ, 3D PDF) and even for 3D printing. The resulting 3D models can be used for multiple applications, including 3D printing for exhibitions, teaching, popularisation, and functional analyses such as mechanical modelling, buoyancy tests, and functional morphology (Clemo and Dorgan, 2017). Due to its efficiency, this method is well-suited for digitising palaeontological collections and for further scientific evaluation.

Micro-CT, on the other hand, provided volumetric data and revealed internal structures inaccessible by photogrammetry. Both scolecodonts and chitinozoans were successfully visualised, confirming that high-resolution laboratory submicron-CT can capture internal and external structure not only of mineralised but also of organic-walled specimens. This subsequently enables virtual exploration of wall thickness (Figure 2, Appendices 1, 2), internal cavities, mineral growth patterns, and voids (Figure 3). Micro-CT is particularly valuable for studying fused polychaete jaw apparatuses (Figure 4, Appendix 3), as individual maxillae and other elements can be digitally separated and examined from different angles, overcoming the challenge posed by overlapping elements that often prevent species-level identification (Appendix 3). The method also provides insights into internal structures that are otherwise difficult to observe: in chitinozoans, wall features such as the prosome or

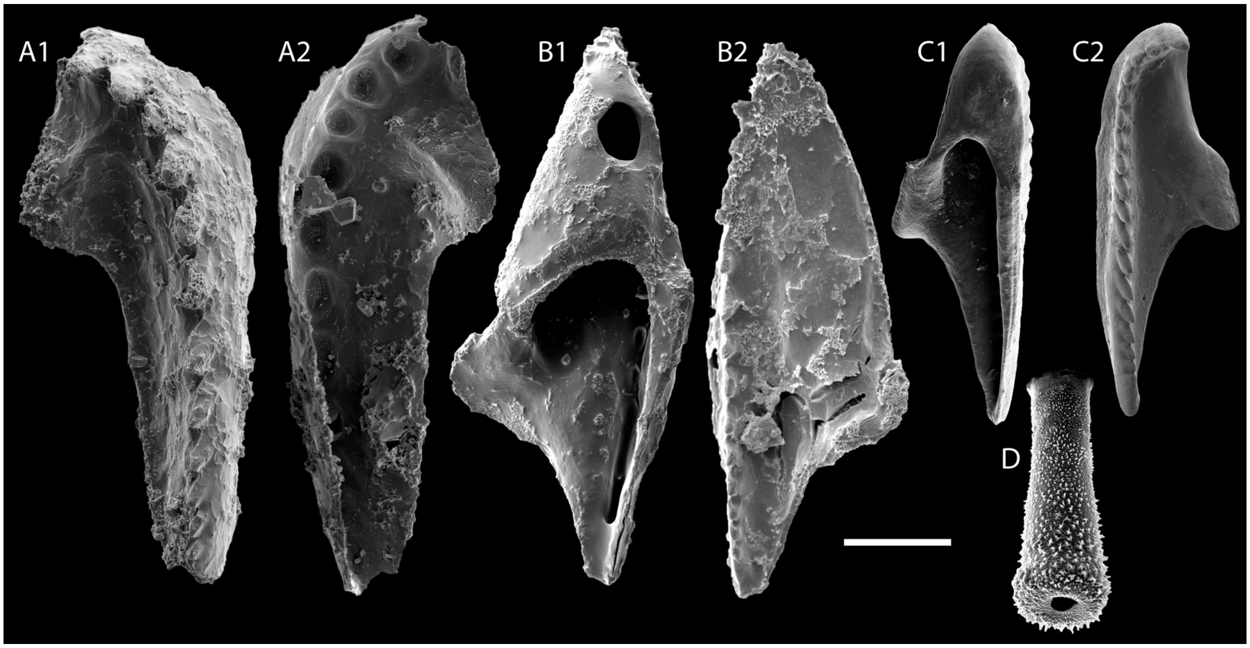

FIGURE 8. SEM photographs used for the SEM-photogrammetry. The scale bar refers to 100 µm. A. *Pistoprion* sp., left first maxilla, specimen PT172_1, sample K57, Kosov Quarry, Czech Republic, A1. Dorsal side. A2. Ventral side. B. *Protarabellites rectangularis*, right first maxilla, specimen PT173_1, sample K57, Kosov Quarry, Czech Republic, B1. ventral side B2. dorsal side. C. *Oenonites* sp. right first maxilla, specimen PT74_1, sample K57, Kosov Quarry, Czech Republic, C1. Ventral side. C2. Dorsal side. D. specimen PT171_4, Saku Quarry, Estonia.

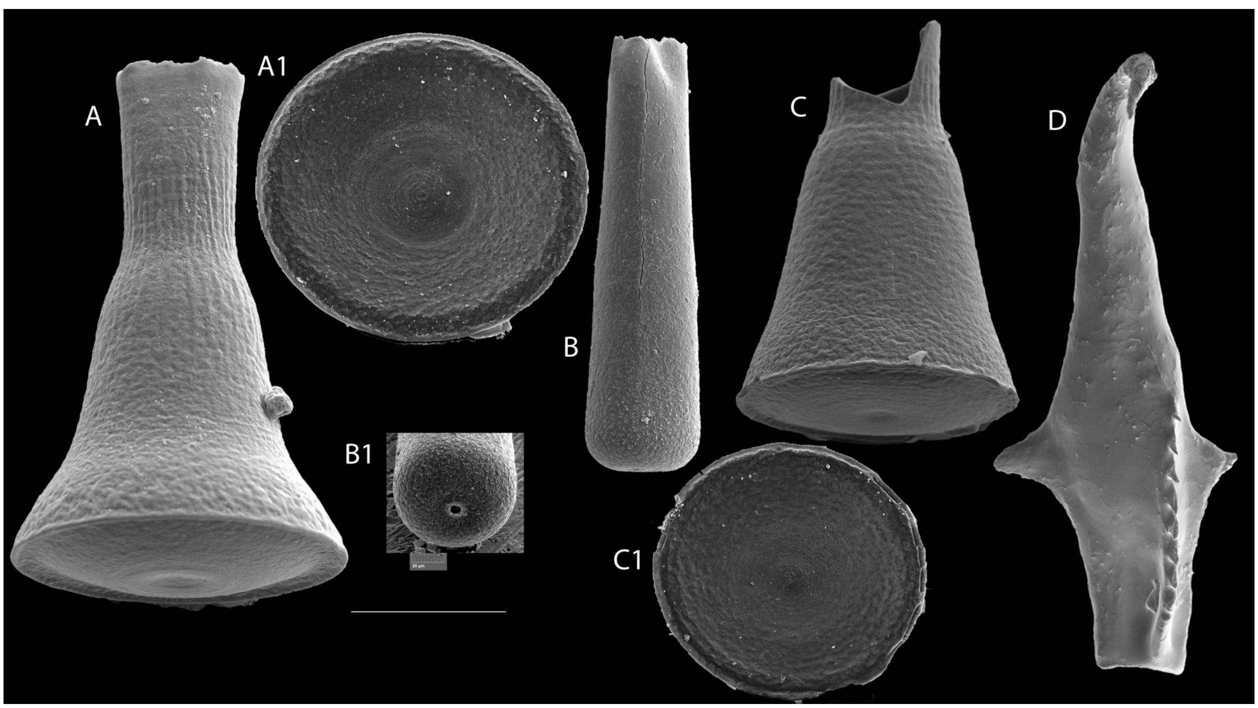

FIGURE 9. SEM photographs of the chitinozoan specimens analysed on the CT. Scale bar represents 100 µm except for figure D, where it represents 125 µm. A. Specimen PT175_1, OM12-6, Sutlema Quarry, Estonia, Saunja Formation, Katian, A1. Detail of aboral side of the specimen A. B. Specimen PT175_3, sample OM12-6, Sutlema Quarry, Estonia, Saunja Formation, Katian, B1 Detail of aboral side of the specimen B. C. Specimen PT175_2, OM12-6, Sutlema Quarry, Estonia, Saunja Formation, Katian, C1. Detail of aboral side of the specimen C. D. *Spitiprion khannai*, left MI, specimen PT169_1, India, Spiti Formation.

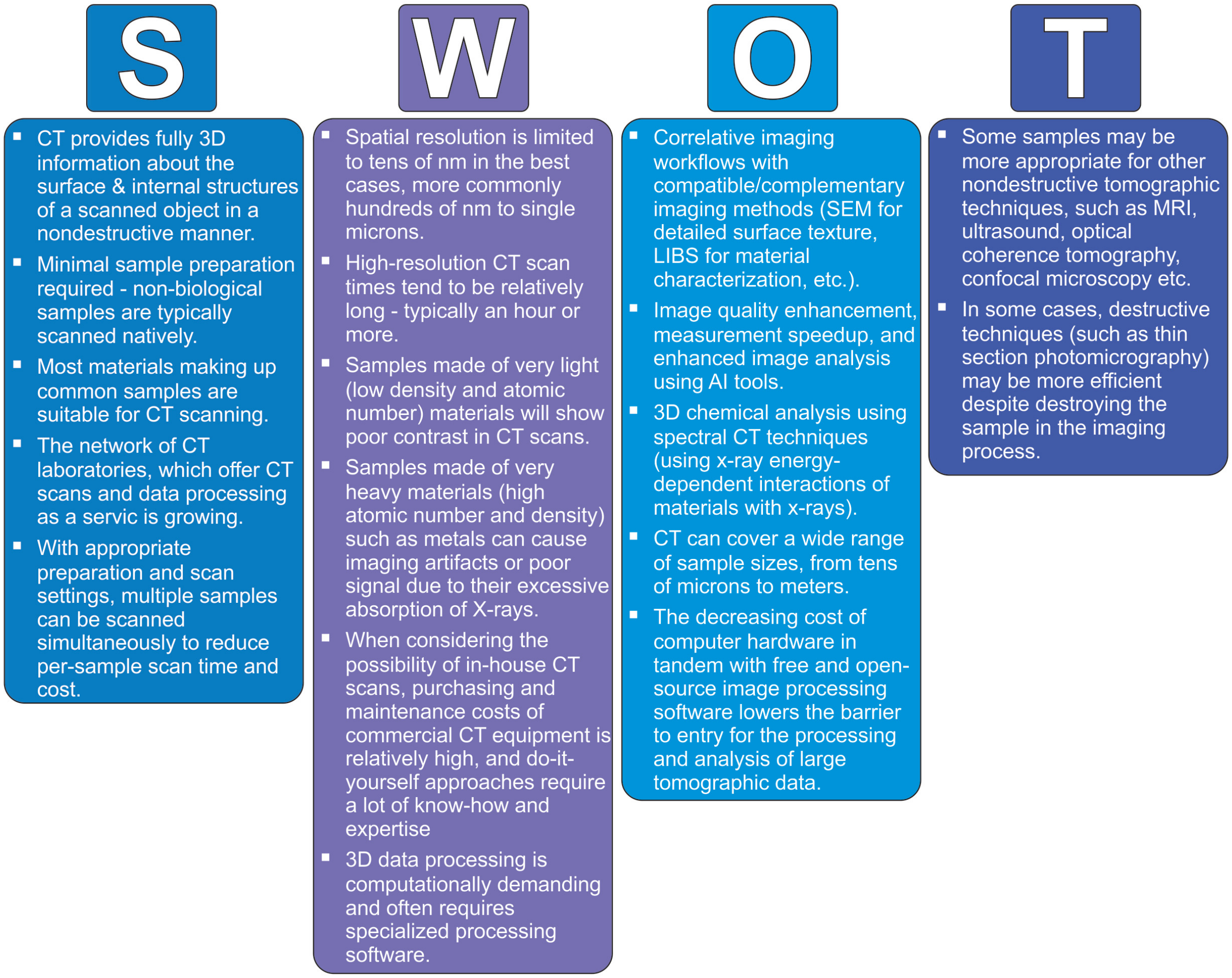

FIGURE 10. SWOT (Strengths, Weaknesses, Opportunities, Threats) analysis of the submicron-CT method.

operculum (Figure 5, Appendices 4–7) are important for higher level systematics, while in scolecodonts, wall characteristics and internal voids (Figures 2, 3) inform on mechanical properties, diet, and functional morphology. For example, voids in the first maxilla, previously reported only in the first maxilla of the genus *Ramphoprion* by Mierzejewska and Mierzejewski (1978), were confirmed in the first maxillae of the genus *Spitiprion*, occurring in the thickest part of the maxilla. These voids contribute to jaw toughness through gradient metal-ligand interactions, creating a hard, energy-absorptive tip and a soft, energy-dissipating base, with cavitation events alleviating stress at failure zones and producing characteristic plateau regions in tensile curves (Lichtenegger et al., 2003; Degtyar et al., 2014; Thompson et al., 2019).

However, some limitations of micro-CT must also be mentioned. Handling and mounting microfossils proved technically demanding; even minimal specimen movement during scanning introduced artefacts that degraded image quality. However, this problem was solved by a new approach to sample attachment using a pipette tip. The achievable resolution of micro-CT, while high, remains lower than that of SEM-based photogrammetry, and image contrast may vary depending on the material composition of samples (compare with SEM photos of the specimens in Figure 9). Furthermore, the high cost of instrumentation, demanding data processing workflow, and large file size pose practical barriers to the routine implementation of this method. Also, advanced operator training and powerful computing resources are required (Paterson et al., 2014; Keklikoglou et al., 2019; Heřmanová et al., 2023).

Overall, micro-CT and SEM-based photogrammetry provide complementary perspectives on microfossil morphology rather than competing alternatives. Micro-CT enables non-destructive

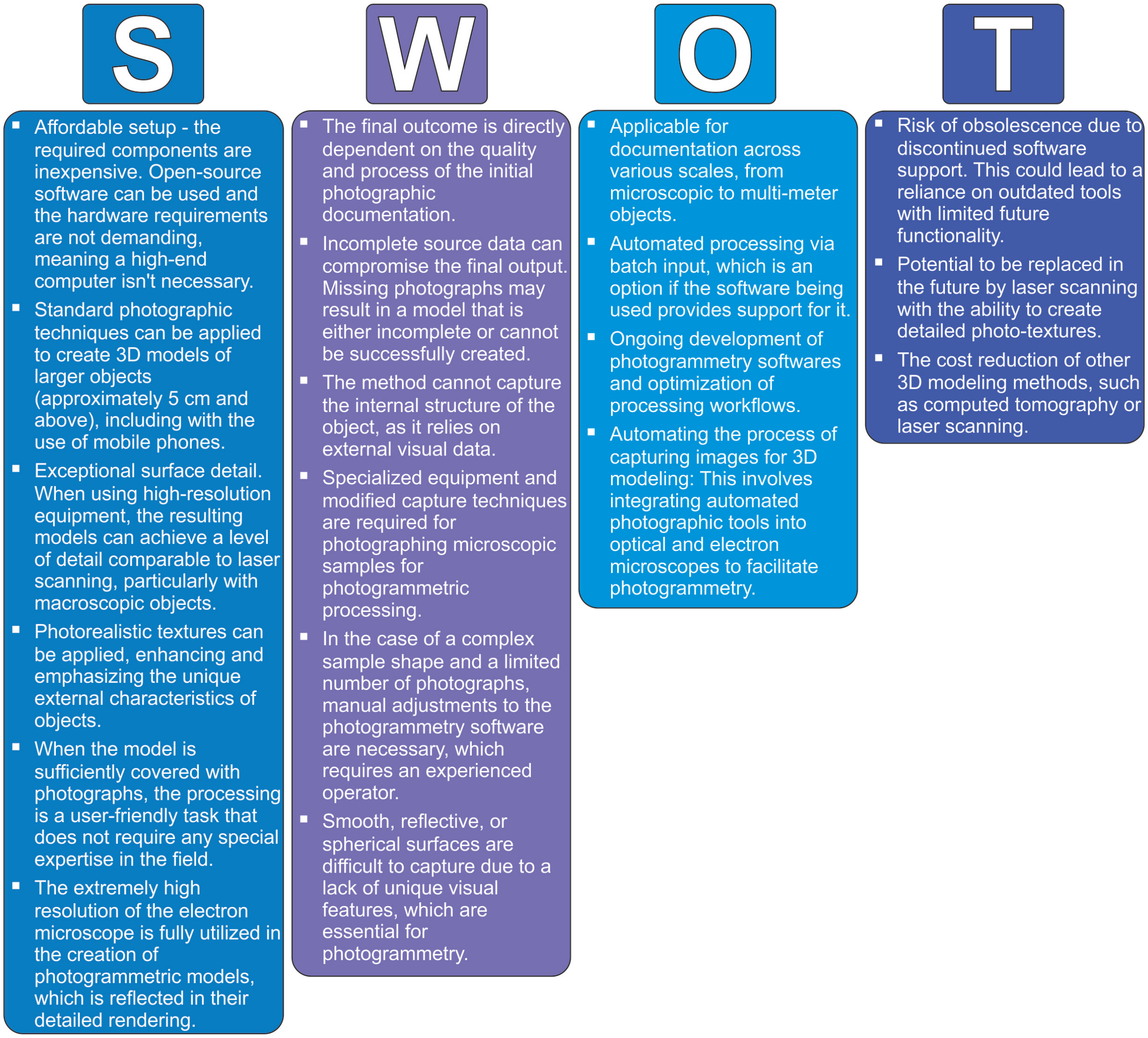

FIGURE 11. SWOT (Strengths, Weaknesses, Opportunities, Threats) analysis of the photogrammetry.

visualisation of internal structures and material heterogeneity, making it essential for functional, structural, and biomechanical analyses. At the same time, photogrammetry offers superior surface resolution and accessibility, ideal for taxonomic documentation. Both techniques can generate digital 3D models suitable for visualisation or 3D printing, enabling use in exhibitions, public education, and functional analyses of the fossils, such as mechanical modelling, buoyancy tests, and studies of functional morphology. Integrating these approaches yields the most comprehensive morphological dataset, capturing both external ornamentation and internal anatomy. Future methodological developments should focus on improving microfossil mounting, automating image reconstruction, and integrating datasets to enhance accessibility, analytical precision, and applicability in palaeontological research.

ACKNOWLEDGEMENTS

We are grateful to two anonymous reviewers and editor N. Nasser for their suggestions that improved the manuscript. We thank the financial support of the Czech Science Foundation, through project No 23-05944K (support to PT), and Brno University of Technology, which provided grant FSI-S-26-9044 (support to JK). We acknowledge CzechNanoLab Research Infrastructure supported by MEYS CR (LM2023051). This is a contribution to the Strategic Research Plan of the Czech Geological Survey (DKRVO/ČGS 2023–2027), the internal project of the Czech Geological Survey No. 311650, and to the IGCP 735.

REFERENCES

Abdelhady, A.A., Seuss, B., Jain, S., Abdel-Raheem, K.H.M., Elsheikh, A., Ahmed, M.S., Elewa, A.M.T., and Hussain, A.M. 2024. New and emerging technologies in paleontology and paleobiology: A horizon scanning review. Journal of African Earth Sciences, 210:105–155. https://doi.org/10.1016/j.jafrearsci.2023.105155

Abel, R.L., Laurini, C.R., and Richter, M. 2012. A palaeobiologist's guide to "virtual" micro-CT preparation. Palaeontologia Electronica, 15:1–17. https://doi.org/10.26879/284

Aber, J.S., Marzolff, I., and Ries, J.B. 2010. Chapter 3 - Photogrammetry, p. 23–39. In Aber, J.S., Marzolff, I., and Ries, J.B. (eds.), Small-Format Aerial Photography. Elsevier, Amsterdam. https://doi.org/10.1016/B978-0-444-53260-2.10003-1

Ball, A.D., Job, P.A., and Walker, A.E.L. 2017. SEM-microphotogrammetry, a new take on an old method for generating high-resolution 3D models from SEM images. Journal of Microscopy, 267:214–226. https://doi.org/10.1111/jmi.12560

Bates, K.T., Breithaupt, B.H., Falkingham, P.L., Matthews, N.A., Hodgetts, D., and Manning, P.L. 2009. Integrated LiDAR & photogrammetric documentation of the Red Gulch Dinosaur Tracksite (Wyoming, USA). Proceedings of the Eighth Conference on Fossil Resources, 101–103.

Bemis, S.P., Micklethwaite, S., Turner, D., James, M.R., Akciz, S., Thiele, S.T., and Bangash, H.A. 2014. Ground-based and UAV-Based photogrammetry: A multi-scale, high-resolution mapping tool for structural geology and paleoseismology. Journal of Structural Geology, 69:163–178. https://doi.org/10.1016/j.jsg.2014.10.007

Bockelie, T.G. 1981. Internal morphology of two species of *Lagenochitina* (Chitinozoa). Review of Palaeobotany and Palynology, 34:149–164. https://doi.org/10.1016/0034-6667(81)90035-X

Boyde, A. and Ross, H.F. 1975. Photogrammetry and the scanning electron microscope. The Photogrammetric Record, 8:408–408. https://doi.org/10.1111/j.1477-9730.1975.tb00805.x

Breithaupt, B.H. and Matthews, N.A. 2001. Preserving paleontological resources using photogrammetry and geographic information systems. In Crossing Boundaries in Park Management: Proceedings of the 11th Conference on Research and Resource Management in Parks and Public Lands. The George Wright Society, Inc.

Clemo, W.C. and Dorgan, K.M. 2017. Functional Morphology of Eunicidan (Polychaeta) Jaws. The Biological Bulletin, 233:227–241. https://doi.org/10.1086/696291

Corradini, D., Russo, F., and Serpagli, E. 1974. Ultrastructure of some fossil and recent polychaete jaws (scolecodonts). Bolletino della Sociéta Paleontologica Italiana, 13:122–134.

Combaz, A., Calandra, F., Jansonius, J., Millepied P., Poumot, C., and Van Oyen, F.H. 1967. Microfossils organiques du Paleozoique, 2, Les Chitinozoaires, Morphographie. Centre National de Recherche Scientifique, Paris, 1–42.

Cunningham, J.A. 2021. The use of photogrammetric fossil models in palaeontology education. Evo Edu Outreach 14, 1. https://doi.org/10.1186/s12052-020-00140-w

Cypionka, H., Voelcker, E., and Rohde, M. 2015. Three simple methods to generate virtual 3D scanning electron micrographs with PICOLAY. Version 28nd February 2015, downloaded 4th October 2025. https://www.picolay.de/SEM3D-tutorial.pdf

Degtyar, E., Harrington, M.J., Politi, Y., and Fratzl, P. 2014. The Mechanical Role of Metal Ions in Biogenic Protein-Based Materials. Angewandte Chemie - International Edition, 53:12026–12044.
https://doi.org/10.1002/anie.201404272

Dinley, J., Hawkins, L., Paterson, G., Ball, A. d., Sinclair, I., Sinnett-Jones, P., and Lanham, S. 2010. Micro-computed X-ray tomography: a new non-destructive method of assessing sectional, fly-through and 3D imaging of a soft-bodied marine worm. Journal of Microscopy, 238:123–133.
https://doi.org/10.1111/j.1365-2818.2009.03335.x

Dumitriu, T., Loghin, S., Brânzilă, M., Baciu, D., Dumitriu, S., Mare, S., Dumitriu, A., and Ionesi, V. 2021. Microscopic “structure-from-motion” photogrammetry, a method for microfossil study. Carpathian Journal of Earth and Environmental Sciences, 16:99–115.
https://doi.org/10.26471/cjees/2021/016/159

Eisenack, A. 1968. Über Chitinozoen des baltischen Gebietes. Palaeontographica Abt. A, 131:137–198.

Eisenack, A. 1972. Beiträge zur Chitinozoen-Forschung. Abt A. Palaeontographica, 140(4/6):117–130.

Eisenack, A. 1976. Weiterer Beitrag zur Chitinozoen-Forschung. Stuttgart. Neues Jahrbuch für Geologie und Paläontologie Monatshefte, 11:641–652.

Eriksson, M.E., Bergman, C.F., and Jeppsson, L. 2004. Silurian scolecodonts. Review of Palaeobotany and Palynology, 131:269–300.
https://doi.org/10.1016/j.revpalbo.2004.04.001

Eriksson, M.E., Hints, O., Paxton, H., and Tonarová, P. 2013. Chapter 18 Ordovician and Silurian polychaete diversity and biogeography. Geological Society, London, Memoirs, 38:265–272.
https://doi.org/10.1144/M38.18

Eriksson, M.E., Parry, L.A., and Rudkin, D.M. 2017. Earth’s oldest ‘Bobbit worm’ – gigantism in a Devonian eunicidan polychaete. Scientific Reports, 7:43061.
https://doi.org/10.1038/srep43061

Eulitz, M. and Reiss, G. 2015. 3D reconstruction of SEM images by use of optical photogrammetry software. Journal of Structural Biology, 191:190–196.
https://doi.org/10.1016/j.jsb.2015.06.010

Falkingham, P.L. 2012. Acquisition of high resolution three-dimensional models using free, open-source, photogrammetric software. Palaeontologia Electronica, 15:15 pp.
https://doi.org/10.26879/264

Faulwetter, S., Vasileiadou, A., Kouratoras, M., Dailianis, T. and Arvanitidis, C. 2013. Micro-computed tomography: Introducing new dimensions to taxonomy. ZooKeys, 263:1–45.
https://doi.org/10.3897/zookeys.263.4261

Girard, C., Charruault, A.-L., Gluck, T., Corradini, C., and Renaud, S. 2022. Deciphering the morphological variation and its ontogenetic dynamics in the Late Devonian conodont *Icriodus alternatus*. Fossil Record, 25:25–41.
https://doi.org/10.3897/fr.25.80211

Gontard, L.C., Schierholz, R., Yu, S., Cintas, J., and Dunin-Borkowski, R.E. 2016. Photogrammetry of the three-dimensional shape and texture of a nanoscale particle using scanning electron microscopy and free software. Ultramicroscopy, 169:80–88.
https://doi.org/10.1016/j.ultramic.2016.07.006

Grahn, Y. 2005. Devonian chitinozoan biozones of Western Gondwana. Acta Geologica Polonica, 55:211–227.

Grahn, Y. 2006. Ordovician and Silurian chitinozoan biozones of western Gondwana. Geological Magazine, 143:509–529.
https://doi.org/10.1017/S001675680600207X

Gueriau, P., Parry, L.A., and Rabet, N. 2023. *Gilsonicaris* from the Lower Devonian Hunsrück slate is a eunicidan annelid and not the oldest crown anostracan crustacean. Biology Letters, 19:20230312.
https://doi.org/10.1098/rsbl.2023.0312

Hay, W. and Sandberg, P. 1967. The Scanning Electron Microscope, a Major Break-through for Micropaleontology. Micropaleontology, 13:407–418.
https://doi.org/10.2307/1484718

Heřmanová, Z., Kočová Veselská, M., Kočí, T., Jäger, M., Bruthansová, J. and Mikuláš, R. 2023. Comparison of methods: Micro-CT visualization method and epoxy cast-embedding reveal hidden details of bioerosion in the tube walls of Cretaceous polychaete worms. Palaeontologia Electronica, 26(2):a18. https://doi.org/10.26879/1255

Hints, O., Tonarová, P., Eriksson, M.E., Rubinstein, C.V., and de la Puente, G.S. 2017. Early Middle Ordovician scolecodonts from north-western Argentina and the emergence of labidognath polychaete jaw apparatuses. Palaeontology, 60:583–593. https://doi.org/10.1111/pala.12303

Jacob, J., Paris, F., Monod, O., Miller, M.A., Tang, P., George, S.C. and Bény, J.-M. 2007. New insights into the chemical composition of chitinozoans. Organic Geochemistry, 38:1782–1788. https://doi.org/10.1016/j.orggeochem.2007.06.005

Jansonius, J. 1964. Morphology and classification of some Chitinozoa. Bulletin of Canadian Petroleum Geology, 12:901–918.

Jansonius, J. 1967. Systematics of the Chitinozoa. Review of Palaeobotany and Palynology, 1:345–360.

Jarochowska, E., Tonarová, P., Munnecke, A., Ferrová, L., and Vodrážková, S. 2013. An acid-free method of microfossil extraction from clay-rich lithologies using the surfactant Rewoquat. Palaeontologia Electronica, 16:1–16. https://doi.org/10.26879/382

Keklikoglou, K., Faulwetter, S., Chatzinikolaou, E., Wils, P., Brecko, J., Kvaček, J., Metscher, B., and Arvanitidis, C. 2019. Micro-computed tomography for natural history specimens: a handbook of best practice protocols. European Journal of Taxonomy, 522:1–55. https://doi.org/10.5852/ejt.2019.522

Kielan-Jaworowska, Z. 1966. Polychaete jaw apparatuses from the Ordovician and Silurian of Poland and a comparison with modern forms. Palaeontologia Polonica, 16:1–152.

Kozikowski, P. 2020. Extracting Three-dimensional Information from SEM Images by Means of Photogrammetry. Micron, 134:102873. https://doi.org/10.1016/j.micron.2020.102873

Laufeld, S. 1974. Silurian Chitinozoa from Gotland. Fossils and Strata, 5:1–130.

Liang, Y., Hints, O., Tang, P., Cai, C., Goldman, D., Nõlvak, J., Tihelka, E., Pang, K., Bernardo, J., and Wang, W. 2020. Fossilized reproductive modes reveal a protistan affinity of Chitinozoa. Geology, 48:1200–1204. https://doi.org/10.1130/G47865.1

Lichtenegger, H.C., Schöberl, T., Ruokolainen, J.T., Cross, J.O., Heald, S.M., Birkedal, H., Waite, J.H., and Stucky, G.D. 2003. Zinc and mechanical prowess in the jaws of *Nereis*, a marine worm. Proceedings of the National Academy of Sciences of the United States of America, 100:9144–9149. https://doi.org/10.1073/pnas.1632658100

Matthews, N.A., Noble T.A., and Breithaupt, B.H., 2006. The application of photogrammetry, remote sensing and geographic information (GIS) to fossil resource management. New Mexico Museum of Natural History and Science Bulletin, 34:119–131.

Melchin, M.J. and Anderson, A.J. 1998. Infrared Video Microscopy for the Study of Graptolites and Other Organic-Walled Fossils. Journal of Paleontology, 72:397–400.

Mierzejewska, G. and Mierzejewski, P. 1975. Breakdown of collagen during phylogenetic development of Polychaeta. Annals of Medical Section of the Polish Academy of Sciences, 20:99–100.

Mierzejewska, G. and Mierzejewski, P. 1977. Electron microscope investigation of the fossil and recent polychaete jaws from the genus Glycera Savigny, 1818. Prace Muzeum Ziemi, Prace Paleozoologiczne, 26:127–130.

Mierzejewska, G. and Mierzejewski, P. 1978. Ultrastructure of the jaws of the fossil and recent Eunicida (Polychaeta). Acta Palaeontologica Polonica, 23:317–339.

Otero, A., Pérez Moreno, A., Falkingham, P., Cassini, G., Ruella, A., Militello, M., and Toledo, N. 2020. Three-dimensional image surface acquisition in vertebrate paleontology: a review of principal techniques. Publicación Electrónica de la Asociación Paleontológica Argentina. https://doi.org/10.5710/PEAPA.04.04.2020.310

Paris, F. 1990. The Ordovician chitinozoan biozones of the Northern Gondwana domain. Review of Palaeobotany and Palynology, 66:181–209. https://doi.org/10.1016/0034-6667(90)90038-K

Parry, L.A., Edgecombe, G.D., Sykes, D., and Vinther, J. 2019. Jaw elements in *Plumulites bengtsoni* confirm that machaeridians are extinct armoured scaleworms. Proceedings of the Royal Society B: Biological Sciences, 286:20191247. https://doi.org/10.1098/rspb.2019.1247

Paterson, G.L.J., Sykes, D., Faulwetter, S., Merks, R., Ahmed, F., Hawkins, L.E., Dinley, J., Ball, A.D., and Arvanitidis, C. 2014. The pros and cons of using micro-computed tomography in gross and microanatomical assessments of polychaetous annelids. Memoirs of Museum Victoria, 71:237–246.

Paxton, H. 2009. Phylogeny of Eunicida (Annelida) based on morphology of jaws. Zoosymposia, 2:241–264. https://doi.org/10.11646/zoosymposia.2.1.18

Popov, D., Roychoudhury, P., Hardy, H., Livermore, L., and Norris, K. 2021. The Value of Digitising Natural History Collections. Research Ideas and Outcomes, 7:e78844. https://doi.org/10.3897/rio.7.e78844

Schwab, K.W. 1966. Microstructures of some fossil and recent scolecodonts. Journal of Paleontology, 40:416–423.

Souquet, L., Corradini, C., and Girard, C. 2020a. *Siphonodella leiosa* (Conodonta), a new unornamented species from the Tournaisian (lower Carboniferous) of Puech de la Suque (Montagne Noire, France). Geobios, 61:55–60. https://doi.org/10.1016/j.geobios.2020.06.004

Souquet, L., Corradini, C., and Girard, C. 2020b. 3D models related to the publication: *Siphonodella leiosa* (Conodonta), a new unornamented species from the Tournaisian (lower Carboniferous) of Puech de la Suque (Montagne Noire, France). Retrieved June 10, 2024, from http://hdl.handle.net/11368/2969440

Strauch, F. 1973. Die Feinstruktur einiger Scolecodonten. Senckenbergiana Lethaea, 1973:1–19.

Surmen, H. 2023. Photogrammetry for 3D Reconstruction of Objects: Effects of Geometry, Texture and Photographing. Image Analysis & Stereology, 42:51–63. https://doi.org/10.5566/ias.2887

Suttner, T.J., Kido, E., and Briguglio, A. 2018. A new icriodontid conodont cluster with specific mesowear supports an alternative apparatus motion model for Icriodontidae. Journal of Systematic Palaeontology, 16:909–926. https://doi.org/10.1080/14772019.2017.1354090

Tasch, P. and Shaffer, B.L. 1961. Study of Scolecodonts by Transmitted Light. Micropaleontology, 7:369. https://doi.org/10.2307/1484371

Thompson, C.B., Chatterjee, S., and Korley, L.T.J. 2019. Gradient supramolecular interactions and tunable mechanics in polychaete jaw inspired semi-interpenetrating networks. European Polymer Journal, 116:201–209. https://doi.org/10.1016/j.eurpolymj.2019.04.015

Tonarová, P., Suttner, T.J., Hints, O., Liang, Y., Zemek, M., Kubajko, M., Zikmund, T., Kaiser, J., and Kido, E. 2024. Late Ordovician scolecodonts and chitinozoans from the Pin Valley in Spiti, Himachal Pradesh, northern India. Acta Palaeontologica Polonica, 69(2):199–215. https://doi.org/10.4202/app.01135.2024

Umnova, N.I. 1973. Methods of Investigation: Use of Infrared Light for the Study of Chitinozoa. Paleontological Journal, 3:394–400.

Urban, J.B. 1972. A reexamination of Chitinozoa from the Cedar Valley Formation of Iowa with observations on their morphology and distribution. Bulletin of American Paleontology, 63:1–43.

Urban, J.B. and Kline, J.K. 1970. Chitinozoa of the Cedar City Formation, Middle Devonian of Missouri. Journal of Paleontology, 44:69–76.

Vodička, J., Muir, L.A., Botting, J.P., Špillar, V., and Fatka, O. 2022. Palaeobiological significance of chitinozoan clusters with parallel vesicles. Marine Micropaleontology, 172:102109. https://doi.org/10.1016/j.marmicro.2022.102109

Wang, W., Liang, Y., Lyu, Q., Hints, O., Chen, S., and Nõlvak, J. 2021. Chitinozoans with “skirt”: Ultrastructure and palaeoecological implications of carina in *Cyathochitina* Eisenack, 1955. Palaeogeography, Palaeoclimatology, Palaeoecology, 570:110348. https://doi.org/10.1016/j.palaeo.2021.110348

Wrona, R. 1980. Microarchitecture of the chitinozoan vesicles and its paleobiological significance. Acta Palaeontologica Polonica, 25:123–163.

APPENDICES

The Appendices for this article are supplied in a zipped file for download.
https://palaeo-electronica.org/content/2026/5926-photogrammetry-in-the-3d-imaging-of-microfossils

APPENDIX 1.

Video, wall thickness mapping of Chitinozoa, acquired by CT scanning, specimen PT175_3, from sample OM12-6, Sutlema Quarry, Estonia, Saunja Formation, Katian.

APPENDIX 2.

Video, wall thickness mapping, acquired by CT scanning, *Spitiprion khannai*, left MI, specimen PT169_1, India.

APPENDIX 3.

Video of the jaw apparatus of *Pistoprion transitans*, acquired by CT scanning, specimen PT176_1, Reinu Quarry, Estonia, Silurian, SM3.

APPENDIX 4.

Video Chitinozoa *Cyathochitina* sp., specimen PT175_1, sample OM12-6, Sutlema Quarry, Estonia, Saunja Formation, Katian. External view of the test from all sides, acquired by CT scanning, an artefact on the specimen due to residual liquid.

APPENDIX 5.

Video Chitinozoa *Cyathochitina* sp., specimen PT175_1, from sample OM12-6, Sutlema Quarry, Estonia, Saunja Formation, Katian, internal view through the test, acquired by CT scanning.

APPENDIX 6.

Video Chitinozoa *Cyathochitina* sp., specimen PT175_2, from sample OM12-6, Sutlema Quarry, Estonia, Saunja Formation, Katian. External view on the test from all sides, acquired by CT scanning. Broken specimen.

APPENDIX 7.

Video Chitinozoa *Cyathochitina* sp., specimen PT175_2, from sample OM12-6, Sutlema Quarry, Estonia, Saunja Formation, Katian. Internal view through the test, acquired by CT scanning.

APPENDIX 8.

Video Chitinozoa external view on the test from all sides, acquired by CT scanning, specimen PT175_3, from sample OM12-6, Sutlema Quarry, Estonia, Saunja Formation, Katian.

APPENDIX 9.

Video Chitinozoa specimen PT175_3, from sample OM12-6, Sutlema Quarry, Estonia, Saunja Formation, Katian. Internal view through the test, acquired by CT scanning, the prosome is visible in the anterior part.

APPENDIX 10.

Video acquired by photogrammetry *Pistoprion* sp., specimen PT172_1, K57, Kosov Quarry, Ludlow, Czech Republic.

APPENDIX 11.

Video acquired by photogrammetry *Protarabellites rectangularis*, specimen PT173_1, K57, Kosov Quarry, Ludlow, Czech Republic.

APPENDIX 12.

Video acquired by photogrammetry *Oenonites* sp., right MI, specimen PT172_1, K57, Kosov Quarry, Ludlow, Czech Republic.

APPENDIX 13.

Three-dimensional pdf acquired by photogrammetry, *Pistoprion* sp., specimen PT172_1, K57, Kosov Quarry, Ludlow, Czech Republic.

APPENDIX 14.

Three-dimensional pdf acquired by photogrammetry, chitinozoa, specimen PT171_4, Saku Quarry, Estonia.

APPENDIX 15.

Obj file acquired by photogrammetry, *Pistoprion* sp., specimen PT172_1, K57, Kosov Quarry, Ludlow, Czech Republic.

APPENDIX 16.

Obj file acquired by photogrammetry, chitinozoa, specimen PT171_4, Saku Quarry, Estonia.

APPENDIX 17.

Three-dimensional pdf acquired by CT scanning, specimen PT175_3, from sample OM12-6, Sutlema Quarry, Estonia, Saunja Formation, Katian.

APPENDIX 18.

Three-dimensional pdf acquired by CT scanning, specimen PT175_1, from sample OM12-6, Sutlema Quarry, Estonia, Saunja Formation, Katian.

APPENDIX 19.

Three-dimensional pdf acquired by CT scanning, specimen PT175_2, from sample OM12-6, Sutlema Quarry, Estonia, Saunja Formation, Katian.